Biophysical Chemistry, 31 (1988) 259–267
Elsevier

BPC 01274

The Fourier transforms of the laser-induced absorption decay from glycogen phosphorylase and DOPA decarboxylase

John W. Ledbetter, John R. Lindroth and Steven M. Martin

Department of Biochemistry and Molecular Biology, Medical University of South Carolina, 171 Ashley Avenue, Charleston, SC 29425, U.S.A.

Received 1 March 1988
Revised manuscript received 25 April 1988
Accepted 25 April 1988

Fourier transform; Laser absorption; Pyridoxal 5′-phosphate; Protein dynamics

Fourier analysis of the laser-induced absorption decay curves of 3,4-dihydroxyphenylalanine (DOPA) decarboxylase and glycogen phosphorylase demonstrates a powerful technique in the analysis of complicated decay behavior. Phosphorylase which uses the pyridoxal 5′-phosphate cofactor in an unknown manner exhibits over weak absorption an intense decay while decarboxylase demonstrates only weak absorption. Fourier analysis of the decay curves clearly shows that phosphorylase has an intense absorption decay in the midst of three weaker ones and that decarboxylase only has three weak decays. This conclusion justifies the isolation and use of the intense decay of phosphorylase as an observable in the study of protein dynamics at the active site about the cofactor. The decay has demonstrated a movement of positive charge to substrate in the mechanism of phosphorylation of glycogen units.

1. Introduction

Cornish and Ledbetter [1] first observed that the ultraviolet energy of a nitrogen laser excites the pyridoxal 5′-phosphate cofactor of glycogen phosphorylase to a transient singlet state. The rate of decay of this state in absorption proved dependent on substrates bound to the enzyme. Refinements to the experiment by Martin et al. [2] demonstrated a more complex decay. A nonlinear least-squares regression procedure returned the best estimates of the parameters in a four-exponential model by converging to a minimum in the sum of squared errors of the data. The method fitted the data to five of the eight parameters of the four-exponential model with convergence. If the initial estimates are too far from the true parameters of a correct model, convergence to a local minimum may result, together with incorrect results. If the model is incorrect, the method will try to fit the data, but may fail to converge. Martin et al. [2] augmented their regression and residual analysis with a knowledge of the photophysics of the cofactor. Both a singlet state involving an intramolecular proton transfer and a triplet state are known products of excitation [3,4]. However, the relative populations of these states for this enzyme are not known.

The Fourier transform analysis of Lindroth et al. [5] supports the two excited-state populations with a total absorbance decay requiring four exponentials. This make credible the separation of the singlet state decay whose rate depends on ligand binding at the active site. The observable increase in this rate constant with substrate phosphate occurs with the movement of protein positive charges away from the cofactor and to the negative substrate [2]. This means that the decay

Correspondence address: J.W. Ledbetter, Department of Biochemistry and Molecular Biology, Medical University of South Carolina, 171 Ashley Avenue, Charleston, SC 29425, U.S.A.

parameters serve as a source of information on the nonclassical role of the cofactor in the phosphorylase mechanism.

This paper presents the Fourier transform results for 3,4-dihydroxyphenylalanine (DOPA) decarboxylase and compares them to those for glycogen phosphorylase. The active site of decarboxylase, which uses pyridoxal 5′-phosphate in a classical fashion, exposes the cofactor to solvent which creates a more hydrophilic environment. In this case, the cofactor does not exhibit an intramolecular proton transfer and, consequently, the transient singlet state. The fluorescence does not have a large Stokes shift. The Fourier analysis shows clearly the difference in the decay behavior of the two enzymes and provides further good evidence for using the singlet state decay of phosphorylase as an observable for dynamic studies.

2. Experimental

The laser excitation experiment has been described previously [2]. A nitrogen laser with emission at 337 nm excites the enzyme. At 90° to the nitrogen laser, a Spectra Physics model 165 continuous-wave Ar^+ laser is pulsed through the sample by a shutter with a programmable interface. The light from the Ar^+ laser passes through a monochromator and registers on an RCA 4526 photomultiplier tube with a 200 Ω load resistance. Data are collected from the photomultiplier tube by the 7A16A vertical amplifier of a Tektronix 7912AD programmable digitizer which digitizes 512 data points over a variable time duration. Signal-averaged data are transferred over a National Instruments IEEE-488 interface bus to an IBM PC/AT where they are converted to absorbance units. The IBM PC/AT was programmed in IBM Professional Fortran for data handling and regression analysis and in Turbo Pascal for the Fourier analysis.

The shutter interface provides programmable control of the shutters during an experiment. The design makes use of a Commodore VIC-20 computer with built-in RS232 software and simple TTL logic circuits. The BASIC program written for the VIC-20 uses a look-up table to decode commands sent over the RS232 bus, and either opens or closes the shutter used for the N_2 laser, or enables or disables pulses produced by a digital delay generator going to the shutter for the Ar^+ laser.

Glycogen phosphorylase *b* was prepared from fresh rabbit muscle by the method of Fischer and Krebs [6]. Assays were in the direction of P_i production. Enzyme concentration in the 2 mM dithiothreitol buffer at pH 6.8 was 1.0 mM in monomer. DOPA decarboxylase was prepared from pig kidney by the method of Borri Voltattorni et al. [7]. Assay procedures followed the method of Sherald et al. [8] and the modifications of Charteris and John [9]. The enzyme concentration in 0.1 M potassium phosphate and 0.1 mM dithiothreitol buffer at pH 6.8 was about 90 mg/ml.

3. Results and analysis

When data appear exponential but the decay model is unknown, a Fourier transform method of analysis can determine the number of exponential components and the decay parameters. No initial estimates and no convergence must be assumed. Therefore, the method offers an advantage over regression techniques for defining or testing a model. The model parameters can then be used as initial estimates for the more precise nonlinear regression analysis. Roesler [10] and Roesler and Pearson [11] introduced the method which is based on the deconvolution properties of the Fourier transform. Two approaches can put the data into a form that can be deconvolved. The more popular method by Gardner et al. [12] transforms data by multiplying each point by its corresponding time value. The second approach, and the one presented here, transforms the data by differentiation [13,14].

The general equation for multicomponent exponential functions,

$$f(t) = \sum_{i=1}^{m} a_i \exp(-k_i t), \tag{1}$$

may be expressed as the Laplace integral equation,

$$f(t) = \int_0^\infty g(k) \exp(-kt)\, dk,$$
$$\text{where } g(k) = \sum_{i=1}^{m} a_i \delta(k - k_i), \tag{2}$$
$$\text{and } \delta(k - k_i) = 1 \quad \text{if} \quad k = k_i$$
$$= 0 \quad \text{if} \quad k \neq k_i$$

is the Kronecker delta. Transformation from $[k,t]$ space to $[x,y]$ space by introducing the logarithmic variables $k = e^{-y}$ and $t = e^x$ results in

$$f(e^x) = \int_{-\infty}^{\infty} g(e^{-y}) \exp(-e^{(x-y)}) e^{-y}\, dy. \tag{3}$$

Differentiation of eq. 3 with respect to x yields

$$df(e^x)/dx = \int_{-\infty}^{\infty} g(e^{-y}) e^{-y} \exp(-e^{(x-y)}) \times (-e^{(x-y)})\, dy. \tag{4}$$

The Fourier transform of eq. 4 is

$$F(\mu) = (1/\sqrt{2\pi}) \int_{-\infty}^{\infty} [df(e^x)/dx] e^{i\mu x}\, dx. \tag{5}$$

Substitution of eq. 4 into eq. 5 and setting $s = x - y$ yields the expression

$$F(\mu) = (1/\sqrt{2\pi}) \int_{-\infty}^{\infty} g(e^{-y}) e^{-y} e^{i\mu y}\, dy \times \int_{-\infty}^{\infty} \exp(-e^s)(-e^s) e^{i\mu s}\, ds. \tag{6}$$

The left integral of eq. 6 is the Fourier transform of $g(e^{-y})e^{-y}$ and the right integral is the Fourier transform of $k(s) = -e^s \exp(-e^s)$. Therefore, eq. 6 may be written as

$$F(\mu) = \sqrt{2\pi}\, G(\mu) K(\mu) \tag{7}$$

which is the Fourier transform of the convolution of $g(e^{-y})e^{-y}$ and $k(s)$ in the time domain. $g(e^{-y})e^{-y}$ is a sum of delta functions of the decay rates and their amplitudes and can be obtained by taking the inverse Fourier transform of eq. 7.

$$g(e^{-y})e^{-y} = (1/\sqrt{2\pi}) \int_{-\infty}^{\infty} (F(\mu)/K(\mu)) e^{-iy\mu}\, d\mu \tag{8}$$

Plotting $g(e^{-y})e^{-y}$ vs. y, which is the equivalent of $g(k)$ vs. k, produces peaks proportional to a_i, the exponential coefficients. The implementation of these transforms was carried out according to Lindroth et al. [5].

Fig. 1 presents the data and results from the differential method of the Fourier analysis. The upper set of graphs represents results for phosphorylase and the lower set is for decarboxylase. The 50 μs/division sweep of the digitizer recorded the data as shown in the upper left of each set. Below that are the transformed data. To the right is the $g(k)$ vs. k spectrum from which the number and rate constants of the decays are determined. In the spectrum of fig. 1A for phosphorylase b, four peaks appear corresponding to four decays. Their amplitudes are proportional to a_i, the exponential coefficients of eq. 1. An intense peak occurs in the midst of three with low amplitudes. The values of k at the maxima (the numbers below the figures) are the rate constants of the exponential decays in μs^{-1}. The Fourier analysis in fig. 1B for DOPA decarboxylase yields a different decay pattern. Three decays are present with the fastest having the highest amplitude and the trailing two at one-half the intensity. The intense peak of phosphorylase does not appear. Unassigned minor peaks, both positive and negative, in the spectra are error ripples due to a finite cutoff value in the inverse Fourier transform. Because they shift position with the cutoff value and are more narrow, they can be discerned from true peaks. Further, the analysis of the data provided for decay lifetimes greater than 1 μs. Decays with lifetimes less than 1 μs, e.g., in the case of the 10 μs/division sweep, would contain less than five data points/lifetime and, therefore, are considered less reliable.

Fig. 2A compares the absorption decay data at 50 μs/division sweep for both phosphorylase b and DOPA decarboxylase. The most notable difference arises in the less intense initial absorption for DOPA decarboxylase and its more intense trailing absorption. Otherwise, the exponential structure of both curves is apparent. To test the model demonstrated by the Fourier analysis, an IMSL, nonlinear least-squares regression subroutine based on the Levenberg-Marquardt al-

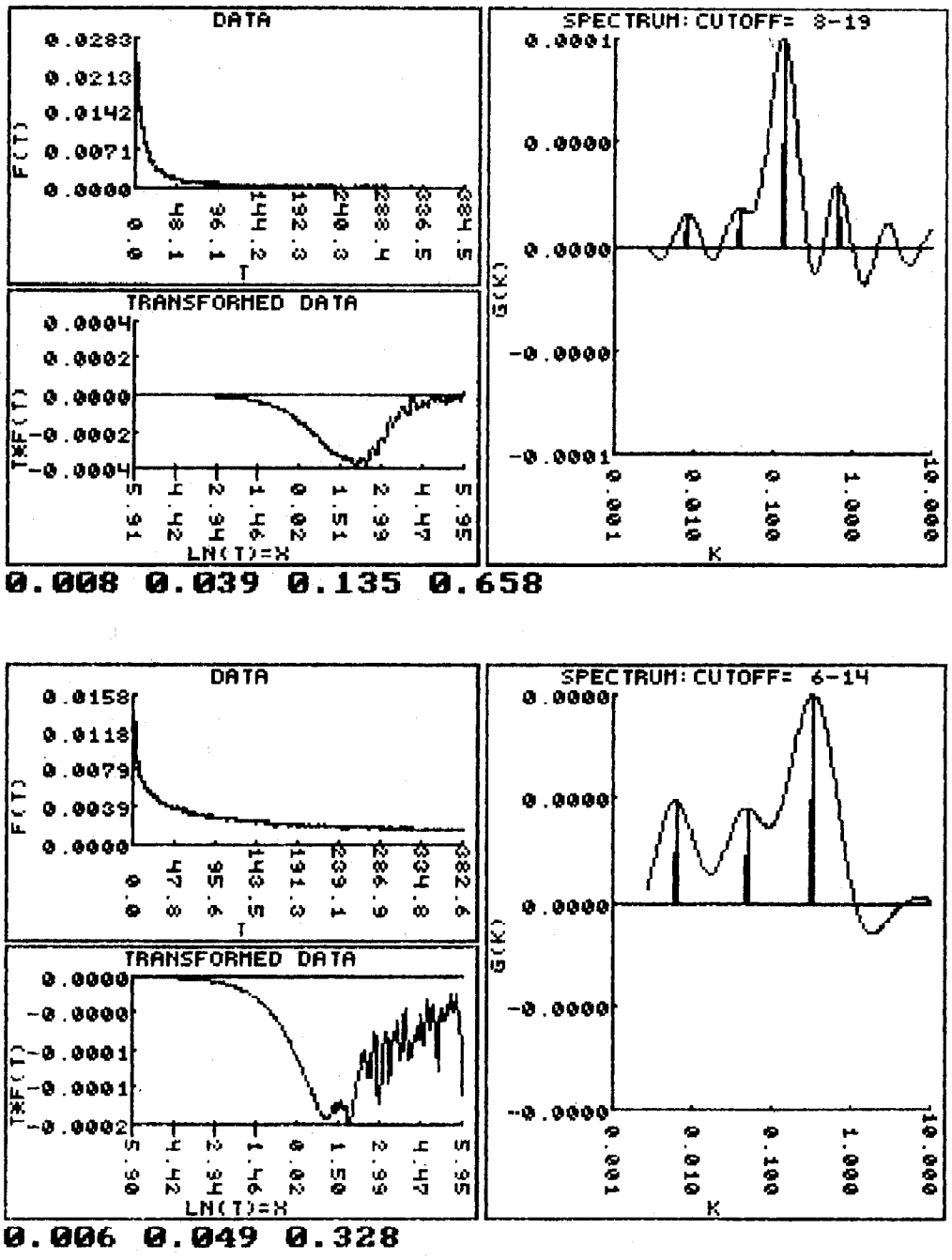

Fig. 1. (A, upper) Application of the differential method of the Fourier analysis to the laser-induced absorption decay curve for glycogen phosphorylase *b*. (B, lower) Same for the DOPA decarboxylase decay curve. 50 μs/division sweep. Values of T are in μs and of k in μs^{-1}. Numbers below each set of figures represent k for each decay found. The amplitude of the peaks in $G(k)$ provides only relative strengths.

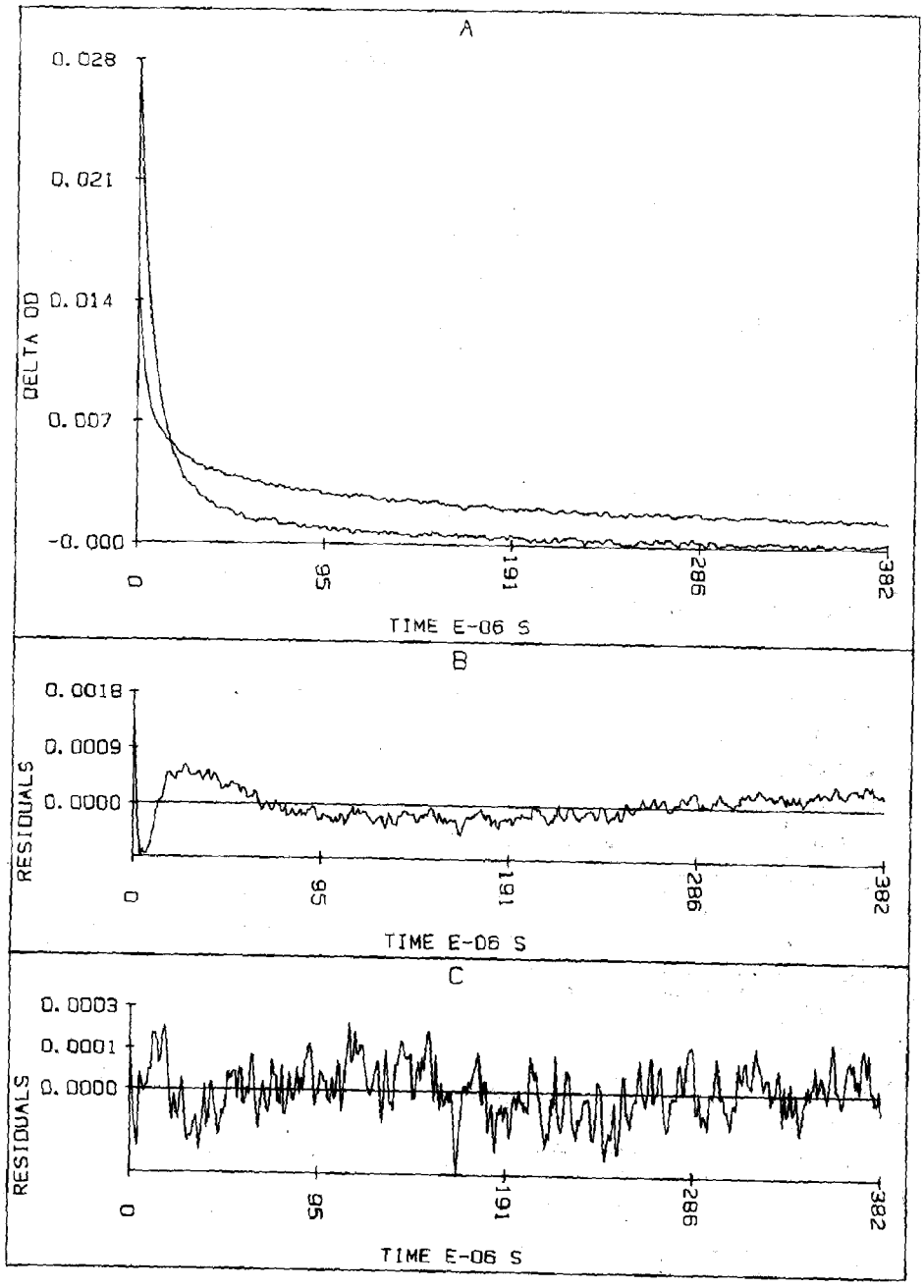

Fig. 2. (A) Laser-induced absorption decay for glycogen phosphorylase *b* (more intense decay) and DOPA decarboxylase at pH 6.8. 50 μs/division sweep. (B) Residuals from a fit of the decarboxylase curve with two exponentials. (C) Residuals from a fit of the decarboxylase curve with eq. 9.

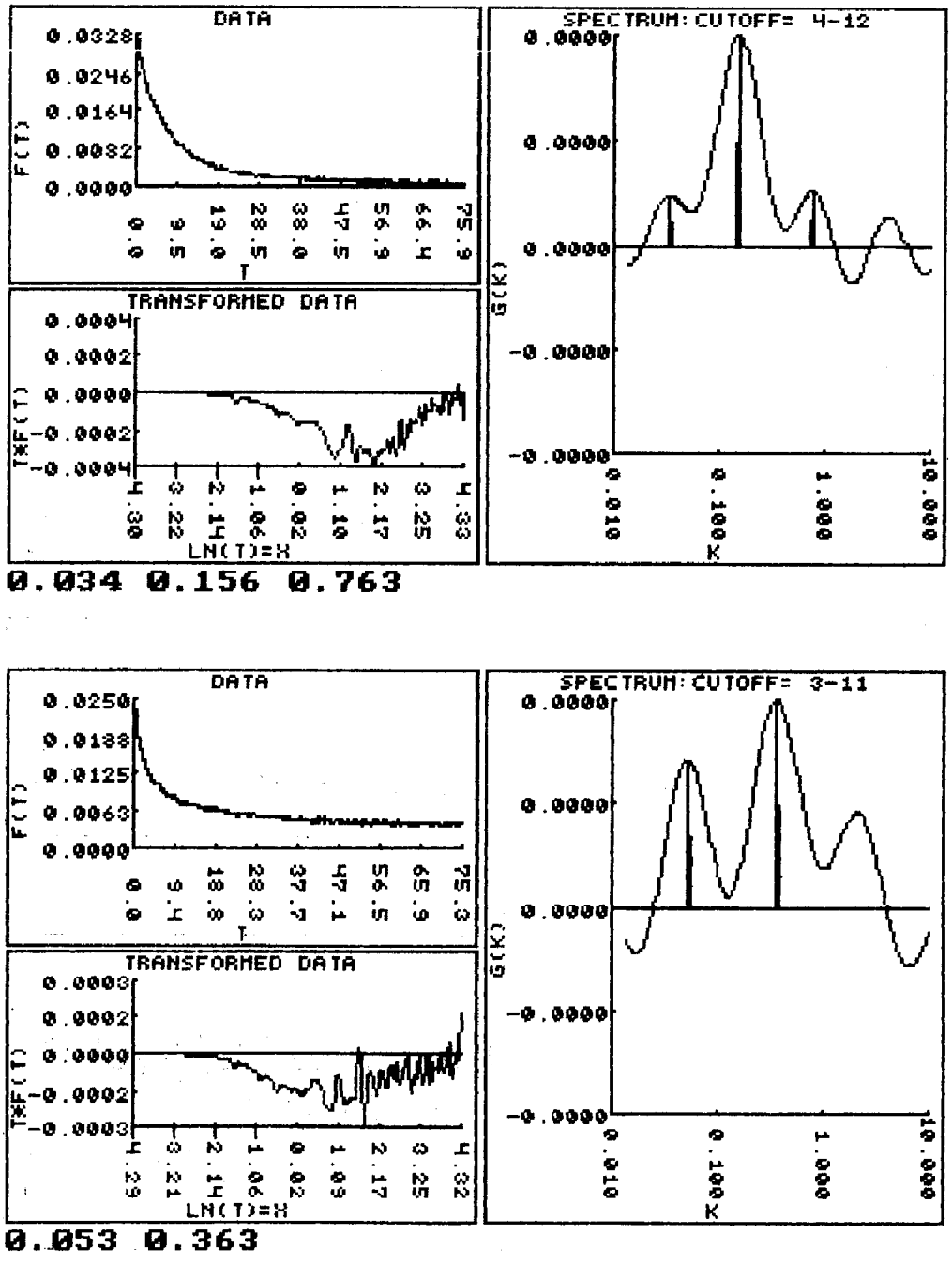

Fig. 3. (A, upper) Fourier analysis of the absorption decay curve for glycogen phosphorylase *b*. (B, lower) Fourier analysis of the DOPA decarboxylase decay curve. 10 μs/division sweep.

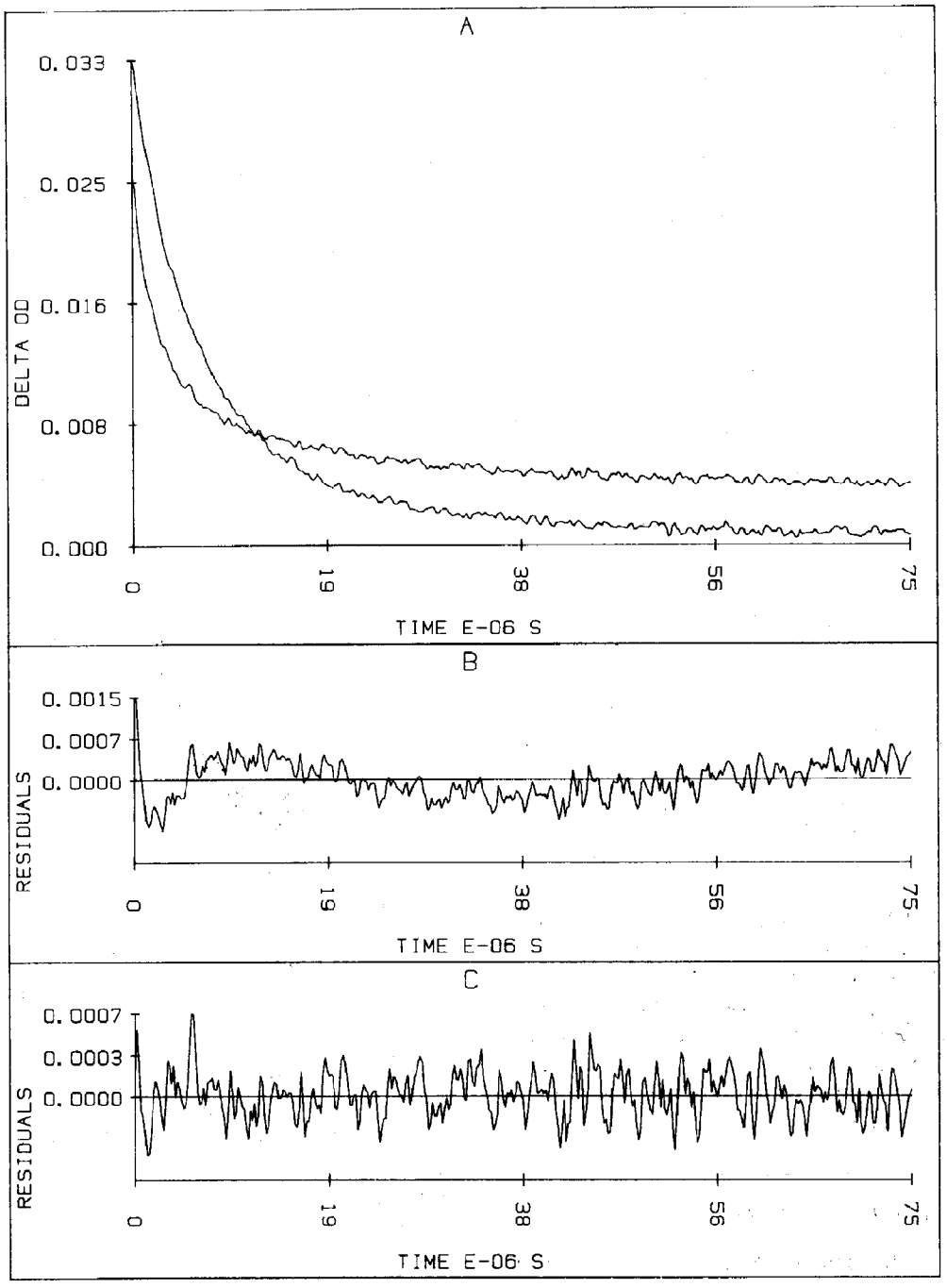

Fig. 4. (A) Laser-induced absorption decay for glycogen phosphorylase *b* (more intense decay) and DOPA decarboxylase at pH 6.8. 10 μs/division sweep. (B) Residuals from a fit of the decarboxylase curve with two exponentials. (C) Residuals from a fit of the decarboxylase curve with eq. 10.

gorithm fitted the Fourier-estimated number of parameters to the data for the decarboxylase. Martin et al. [2] have reported the regression results for phosphorylase. Fig. 2B demonstrates an unsatisfactory fit of the decarboxylase curve with fewer than the Fourier-estimated parameters, i.e., two exponentials. Note the disagreement at short and long times. Using all the Fourier decay constants as input parameters, the fit in fig. 2C with three exponentials shows significant improvement in the random residuals.

$$A(t) = 0.009 \exp(-250\,000t) + 0.004 \exp(-25\,000t) + 0.003 \exp(-1800t) \quad (9)$$

To provide more data points/lifetime for the faster decays, the experiment was repeated at 10 μs/division sweep. The Fourier analysis of fig. 3 will not contain the longest decay because it was not observed for the required time, but the decay patterns of the faster decays agree with the respective ones of fig. 1. Three decays occur for phosphorylase with the second fastest being the most intense. Two decays remain for DOPA decarboxylase with the fastest having the highest amplitude. This agrees with the results for the sweep at 50 μs/division and supports the argument for different decay modes.

The decays of phosphorylase and decarboxylase at 10 μs/division are compared in fig. 4A. Again, to demonstrate a poor fit with fewer than the Fourier estimates, a two-exponential fit of the fast sweep for DOPA decarboxylase yields the residuals of fig. 4B. Because the 50 μs/division sweep shows a long decay at 1800 s^{-1}, a three-exponential fit of decarboxylase, holding $k = 2000$ s^{-1}, produces a good fit as shown by the random residuals of fig. 4C.

$$A(t) = 0.013 \exp(-484\,000t) + 0.007 \exp(-70\,000t) + 0.005 \exp(-2000t) \quad (10)$$

At fast sweeps the short lifetimes will contain more data points so that the large rate constants of eq. 10 will be more reliable.

4. Conclusion

The decay of the transient absorption of DOPA decarboxylase and phosphorylase *b* induced by the ultraviolet laser clearly shows different behavior. Phosphorylase *b* exhibits an intense absorption decay overlapped by three much weaker decays. DOPA decarboxylase shows only the three weak decays. It is likely that these weak decays have a common origin in a triplet state decay mechanism but that has not been proved. What is clear is that phosphorylase *b* shows evidence of the singlet state that results from a proton transfer in the excited state. Förster [15] and Weller [16] showed that the hydroxyl proton on a phenol is more labile in the excited state. Fluorescence data give a pK_a value for the cation of the hemiacetal form of pyridoxal in the excited state of -3.3 [17]. The ground state value is 4.2 [18]. Therefore, excitation of the cofactor in phosphorylase *b* will increase the acidity of the 3-OH group by 10^7-times. In the excited state this proton migrates within 5 ps [19] to the imine nitrogen of the Schiff base which becomes more basic. Clear evidence that the proton transfer occurs in phosphorylase *b* exists in the large Stokes shift of its fluorescence [20]. When the molecule loses the electronic energy, the back-transfer of the proton requires microseconds. This lower transient singlet state is the source of the intense absorption and decay observed at 470 nm. This lower state with the proton on the imine nitrogen and the ionized 3-O provides a strong dipolar structure in a hydrophobic environment. The stability of this structure will be very sensitive to the conformation of protein groups about it.

At pH 7.0 phosphorylase *b* has an $A_{333}:A_{425}$ ratio of 13.3 which means that the cofactor exists largely in the enol form [20]. The ratio for DOPA decarboxylase at pH 6.8 is 3.5–3.8 [21]. One might expect, therefore, some enol structure with its large Stokes-shifted fluorescence and transient absorption. According to Borri Voltattorni et al. [7] only feeble emission occurs at 490 nm when excited at 420 nm and not at 335 nm. No singlet state transient absorption was observed. If the cofactor is removed from DOPA decarboxylase, an absorption shoulder remains at 330 nm. Excita-

tion of this absorption with the ultraviolet laser produces transient absorption similar to that for holoenzyme (J.W. Ledbetter and S.M. Martin, unpublished results). Concerns arise, therefore, over how much of the absorbance at 335 nm represents enol structure, the resolution procedure and how the cofactor binds to the enzyme. Continued studies address the information contained in the decay measurements on the cofactor in DOPA decarboxylase.

This comparison of the phosphorylase and decarboxylase enzymes justifies the separation of the intense laser-induced absorption decay of phosphorylase from other absorption for observations of the effect of substrates on the protein dynamics.

Acknowledgments

This research was partially supported by U.S. Department of Health and Human Services Grant GM 33409 and by a grant from the South Carolina State Appropriation for Biomedical Research. The work was presented at the 1987 Vitamin B6 Congress in Turku, Finland.

References

1 T.J. Cornish and J.W. Ledbetter, Eur. J. Biochem. 143 (1984) 63.
2 S.M. Martin, J.R. Lindroth and J.W. Ledbetter, Biochemistry 25 (1986) 6070.
3 T.J. Cornish and J.W. Ledbetter, IEEE J. Quantum Electron. QE-20 (1984) 1375.
4 T.J. Cornish and J.W. Ledbetter, Photochem. Photobiol. 41 (1985) 15.
5 J.R. Lindroth, S.M. Martin and J.W. Ledbetter, Comput. Biol. Med. 17 (1987) 369.
6 E.H. Fischer and E.G. Krebs, J. Biol. Chem. 231 (1958) 65.
7 C. Borri Voltattorni, A. Minelli, P. Vecchini, A. Fiori and C. Turano, Eur. J. Biochem. 93 (1979) 181.
8 F.A. Sherald, C.J. Sparrow and F.T. Wright, Anal. Biochem. 56 (1973) 300.
9 A. Charteris and R. John, Anal. Biochem. 66 (1975) 365.
10 F.C. Roesler, Proc. Phys. Soc. Lond. B, 68 (1955) 89.
11 F.C. Roesler and J.R.A. Pearson, Proc. Phys. Soc. Lond. B, 67 (1954) 338.
12 D.G. Gardner, J.C. Gardner, G. Lausch and W.W. Meinke, J. Chem. Phys. 31 (1959) 978.
13 D.N. Swingler, IEEE Trans. Biomed Eng. BME-24 (1977) 408.
14 A. Mikkelsen, B.T. Stokke and A. Elgsaeter, Int. J. Bio-Med. Comput. 16 (1985) 35.
15 T. Förster, Naturwissenschaften 36 (1949) 186.
16 A. Weller, Prog. React. Kinet. 1 (1961) 187.
17 J.W. Bridges, D.S. Davies and R.T. Williams, Biochem. J. 98 (1966) 457.
18 D.E. Metzler and E.E. Snell, J. Am. Chem. Soc. 77 (1955) 2431.
19 P.F. Barbara, P.M. Rentzepis and L.E. Brus, J. Am. Chem. Soc. 102 (1980) 2786.
20 S. Shaltiel and M. Cortijo, Biochem. Biophys. Res. Commun. 41 (1970) 594.
21 C. Borri Voltattorni, A. Minelli and C. Turano, FEBS Lett. 17 (1971) 231.